# EXPERIMENTAL AND NUMERICAL ANALYSIS OF A THERMOSYPHON SOLAR WATER HEATER FOR DOMESTIC APPLICATIONS

Basim FREEGAH[1], Aouf A. Al-TABBAKH[2]

*An experimental and numerical Study is carried out on a solar water heater working in thermosyphonic mode. The heater consists of a flat-plate solar collector, a heat exchanger, a storage tank and the connecting piping. Water is the working fluid that flows in a closed loop where it heats up in the solar collector risers and delivers its collected heat to the water storage tank via an immersed heat exchanger. Experiments were carried out in indoor tests using artificial halogen lamps as an alternative to solar radiation. The Numerical work was performed using CFD techniques and a commercial computer software. Semi-empirical formula was proposed to estimate thermosyphonic mass flow rate. The effects of various geometric and performance parameters were considered which include: number of risers, riser length-to-diameter ratio and solar heat flux patterns. A constant heat flux of 500 W/m$^2$ was applied to the collector from four artificial halogen lights for five hours. Maximum tank temperature of 34$^o$C was reached with a nearly constant thermosyphonic mass flow rate of 0.0035 kg/s. Results can be used as a design tool in initial sizing and evaluation of solar water heaters for domestic applications.*

**Keywords**: Solar Water Heaters, Thermosyphon, Flat-Plate Collector, CFD

## 1. Introduction

Solar Water Heaters (SWHs) are the most feasible equipments to harness solar energy for domestic and industrial applications. A variety of designs were proposed and produced in the last four decades. All these designs include a collection unit (solar collector) and a storage unit (tank). The working fluid is circulated between the collector and tank by one of two means: - forced circulation via a mechanical pump or natural circulation without a pump. In natural circulation SWHs (referred to as thermosyphon SWHs) the working fluid (water) is circulated due to the difference in buoyancy forces between the storage tank and the solar collector. This difference is established as a result of temperature difference between the cold region inside the tank with a higher

[1]Assc. Prof., Dept.of Mechanical Eng., Al-Mustansiriyah University, Baghdad, Iraq, e-mail: basimfreegah@yahoo.com
[2]Assc. Prof., Dept.of Mechanical Eng., Al-Mustansiriyah University, Baghdad, Iraq, e-mail: aoufaltabbakh72@gmail.com

density and the hot region in the collector with less density. The tank level should, therefore, be higher than the solar collector level.

One of early studies on thermosyphon solar water heaters was carried out by D. J. Close (1962) [1], who developed a theoretical method to estimate the thermal performance of the heater and conducted experimental measurements to validate the study. Gupta and Garg (1968) [2] refined Close's model by considering thermal capacity of the system and absorber plate efficiency factor. This modification made the model more effective in transient operation representation. Ong K. S. in his two studies; (1974) [3] and (1976) [4], was the first to apply Finite Difference Method on solar water heaters. He used a model similar to that of Close [1] and Gupta and Garg [2] in assuming single representative temperature of the system. The variation of heat transfer coefficients and water properties with temperature was accounted for in Ong's Studies. Other important studies [5-9] appeared later and adopted more elaborated theoretical and experimental techniques to analyze thermosyphon solar water heaters.

The widespread use of solar water heaters necessitated a standard method for testing and rating of these systems. Huang (1993) [10] developed a method for rating thermosyphon solar water heaters. The method depends on a characteristic efficiency to rate different systems. This efficiency is derived by linear regression analysis of large number of test data.

Other designs appeared later like the use of mantle heat exchanger between the thermosyphon cycle and water storage tank. The mantle heat exchanger surrounds the external wall of the tank so that the heat transfers inwards to the tank. Morrison et al. (1998) [11] conducted experimental and numerical study on a thermosyphon solar water heater incorporating mantle type heat exchanger. The effects of various parameters affecting the system were studied like the flow patterns in the annular space of the heat exchanger and the location of the inlet ant outlet ports. The horizontal orientation of the tank along with the presence of the mantle heat exchanger degrades thermal stratification in the inner tank. The inner tank temperature was kept constant in the analysis.

The rapid advancement of computers and numerical techniques in recent years stimulates the researchers to adopt more elaborate theoretical and numerical techniques in studying thermosyphon solar water heaters. The focus included various aspects and configurations. Belessiotis and Mathioulakis (2002) [12] studied simple domestic solar water heater without heat exchanger (direct type). Koffi et al. (2008) [13] dealt with a system equipped with internal heat exchanger of the rolled copper type. Kalogirou (2009) [14] related the thermal performance of thermosyphon solar water heaters with economic and environmental life cycle analysis. Subramanian et al. (2012) [15] analyzed the solar water heating system using CFD methods which were verified experimentally. The work studied the effects of header diameter on system performance. Zelzouli et al. (2014) [16] considered long term operation in their numerical and experimental study. Finally, a detailed dynamic model was developed by Tse and Chow (2015) [17] which handled a system with internal heat exchange coil of the circular tube rings type. A review on the development of domestic solar hot water systems is given by Srinivas (2011) [18].

The solar collector is the main part in any solar water heater. As a result, many researchers studied a variety of aspects regarding the performance of solar collectors. Kundu (2002) [19] carried out a comparative numerical study on flat-plate collector absorbers of different profiles, namely; rectangular, trapezoidal and rectangular with a step change in local thickness (RPSLT). The results showed that the RPSLT profile of absorber plate is superior to other profiles and easier to fabricate. However, the author did not take the effect of changing amounts of working fluid within the system into consideration. Furthermore, the system performance was not compared with the performance of the traditional systems. Varol and Oztop (2008) [20] conducted a comparative numerical investigation between two collectors with different types of absorbers, namely, a wavy absorber and a flat absorber. In wavy absorbers; the cross section of the absorber plate takes the form of a wave with consequent concave and convex parts. The authors studied the effects of various parameters, which included tilt angle, wave length (the concave-convex pitch distance) and aspect ratio (collector length-width ratio). The results showed a significant effect of shape and tilt angle on natural convection heat inside the solar collectors risers. Sivakumar et al. (2012) [21] compared the performance of a solar collector with two arrangements of the copper riser pipes, the traditional straight riser and the zigzag shaped riser. The effect of changing the number of risers was also taken into account. The results showed that increasing the number of risers has a positive effect on the performance. The maximum efficiency reached was 59.09% for 12 risers. Zigzag arrangement further increased the collector efficiency up to 62.90%. However, this study was conducted under no loading conditions. Amori and Jabouri (2012) [22] conducted a comparative study between two types of solar collectors; one with a traditional absorber and the other with an accelerated absorber which is a new design of absorbers. In accelerated absorbers the risers have entrance cross sectional area that is greater than exit area (converging risers). The performance test was carried out in identical conditions for both types and maintaining a tilt angle of $33^{o}$ facing south. The results showed a significant improvement in thermal performance for the new design compared with the traditional type. The temperatures of the storage tank for the new and conventional types were $50^{o}C$ and $37^{o}C$ respectively.

Despite the large volume of literature devoted to analyzing and experiment solar water heaters; some important parameters like the number of risers, length-to-diameter ratio of the riser and intermittent heat flux were not fully accounted for. Most of the research work was devoted to systems with direct circulation of tank water in the solar collector. Solar heaters with a heat exchanger inside water storage tank were not fully accounted for. The accurate measure and estimation of thermosyphonic mass flow rate is still controversial in the literature. Furthermore, the CFD techniques are still not widely incorporated in modeling solar water heaters. Accordingly, the present work endeavors to fill the research gaps in the aforementioned areas through an experimental study backed by CFD modeling of a thermosyphon solar water heater with a heat exchanger inside water storage tank. Such a system is likely to be used when anti-freeze solution is circulated in the solar collector or when a single collector serves several storage tanks. Semi-empirical relationship was, also, developed to estimate thermosyphonic mass flow rate.

## 2. Experimental rig

An experimental setup was manufactured and tested at the labs of University of Huddersfield in UK. The rig consists of the following components (Figs. 1-3):

a. Flat plate solar collector having 5 risers.
b. Water storage tank.
c. Heat exchanger plunged inside the tank.
d. Upriser to collect the heated water from the five risers.
e. Downcomer to return the water from the heat exchanger and distribute it back to the five risers.
f. Four halogen lamps to simulate the solar radiation.
g. Seven thermocouple probes to measure the temperature at the inlet and exit of the collector, at four points in the absorber plate and at the water storage tank.
h. Data acquisition system connected to a computer.

Table (1) shows the specification of the system under consideration.

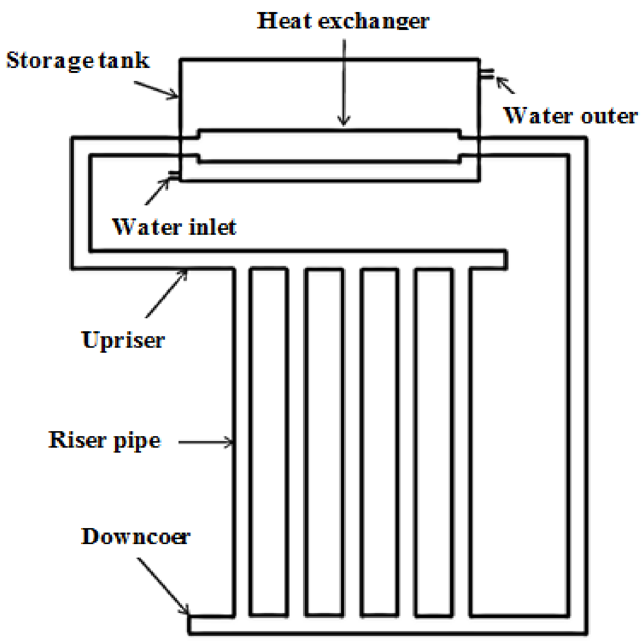


Fig. 1: Schematic view of the thermosyphon system under consideration.

*Table 1*

**Specifications of the system under consideration** (*all dimensions in meters*).

| Item | Dimension or material |
|---|---|
| Height of casing | 1.2 |
| Width of casing | 1.1 |
| Depth of casing | 0.18 |
| Tilt angle of collector | 53º |
| Number of riser pipes | 5 |
| Length of the riser pipes | 1 |
| Inside the riser pipe diameter | 0.0136 |
| Outside the riser pipe diameter | 0.015 |
| Riser pipe material | Copper |
| Absorber plate length | 1 |
| Absorber plate width | 1 |
| Absorber plate thickness | 0.0007 |
| Absorber plate material | Copper |
| Diameter of tank | 0.398 |
| High of tank | 0.635 |
| Material of tank | Plastic |
| Inside diameter of heat exchanger | 0.0202 |
| outside diameter of heat exchanger | 0.022 |
| Length of heat exchanger | 0.6 |
| Heat exchanger material | Copper |

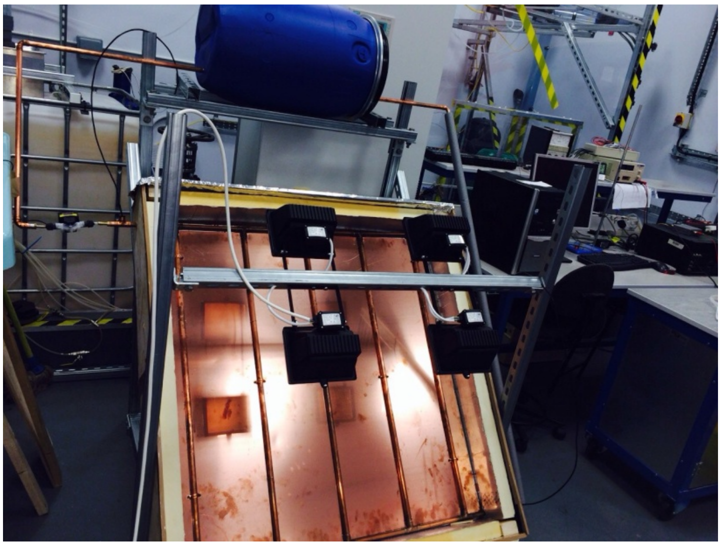

Fig. 2: Photograph of the system under consideration.

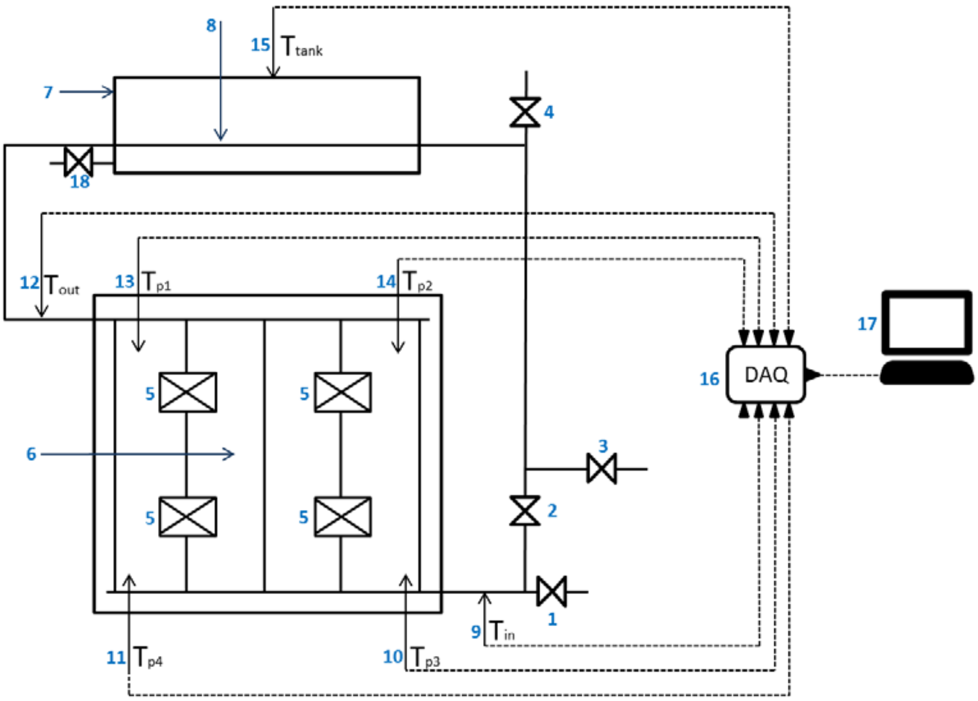


Fig. 3: Schematic view of the thermosyphon loop where: (1 – 4) are valves, (5): Halogen lamps, (6) absorber plate, (7) water storage tank, (8) heat exchanger, (9 – 15) thermocouple probes, (16) data acquisition system, (17) computer and (18) hot water outlet port.

### 3. Modeling Thermosyphonic Mass Flow Rate

The thermosyphonic mass flow rate is generally very low to measure using conventional devices. Any internal device can obstruct the passage of flow and causes serious error in mass flow rate reading. In the present study a new method is proposed to measure mass flow rate depending on the collector inlet and outlet temperatures, water kinematic viscosity and riser diameter. The method is based on relating the mass flow rate of water through the collector risers with collector inlet and outlet temperatures and water kinematic viscosity. A known value of mass flow rate is circulated in the collector risers in an open loop where the collector is separated from the rest of system components. A constant value of heat flux is applied on the collector and the temperature is measured at the collector inlet and outlet after 15 minutes of exposure. The test is repeated several times by varying the value of mass flow rate, collector inlet temperature and heat flux. The data from these tests are used to formulate an equation relating mass flow rate with temperature. Kinematic viscosity and riser diameter are included in the proposed equation to account for the type of the fluid and the riser diameter on the value of mass flow rate. After formulating the equation; it can be used to estimate the thermosyphonic mass flow rate by measuring the collector inlet and outlet temperature. The proposed equation takes the following form:

$$\dot{m} = 189.498 * D * \mu * \left(\frac{T_{out}}{T_{in}}\right)^{1.19} \quad (1)$$

Where D is the riser diameter, μ is the kinematic viscosity and $T_{in}$ and $T_{out}$ are the collector inlet and outlet temperatures in $^{o}C$.

### 4. Experimental Procedure

The thermosyphon loop consisting of the collector risers, the heat exchanger and the connecting pipes, is filled with water through valve (3) (Fig. 3). It is important to expel any air from the loop. This is done by opening valve (4) during the filling until water comes out of it. Water storage tank is also filled through valve (18).

Indoor tests are carried out by applying artificial light from 4 halogen lamps. Each lamp consumes 500 W of electric power and is placed inside a reflective casing of dimensions (16×18 cm). However, the effective power received by the collector absorber plate is less than that emitted by the halogen lamps; rather it depends on the light-absorber distance and the size of the reflective casing of each lamp. The four lamps are fixed at a distance of 30 cm from the absorber. The lamps are spaced by 50 cm in both horizontal and vertical dimensions to ensure equal distribution of the light on an area of 1 $m^2$ which is the absorber area. A digital solar meter (Letron brand – accuracy ±10 $W/m^2$) is used to measure the effective light reaching the absorber and is placed parallel to the glass cover above the absorber. The intensity of the light is regulated by an electric variac to attain the required heat flux on the absorber.

Heat flux is applied in three modes; namely, constant, intermittent and real heat flux. In constant mode; a constant value of 500 $W/m^2$ is applied for five hours. In intermittent mode, the period is extended to seven hours with on-off intervals as given in table 4. The intermittent mode is an approximate representation of the solar radiation in cloudy weather. The duration of sunny and cloudy periods may take endless situations. In the present study a model of 90 minutes of sunny condition (heat flux of 500 $W/m^2$) followed by 15 minutes of cloudy condition (zero heat flux) is used in the software to simulate the intermittent heat flux condition. The pattern is repeated four consecutive times as shown in table (4). The real mode simulates the actual solar radiation at the site of Huddersfield on $15^{th}$ of March as a characteristic day. The solar radiation data were borrowed from local meteorological bureau as an average value of the last five years for the day $15^{th}$ of March. The tests were carried out only for constant heat flux condition to validate the numerical results. The intermittent and real modes were only numerically studied after verifying the software experimentally using the constant heat flux. Quasi-steady state condition is assumed during each time interval which is a reasonable assumption in solar energy related practice to approximate the inherent transient condition of solar radiation.

To carry out the tests, the Halogen lamps are turned on facing the solar collector. The variac is adapted to regulate the intensity of the lamps until the solar meters reads 500 $W/m^2$. Water temperatures at collector inlet and outlet and inside storage tank are measured using K-type thermocouples (±1°C accuracy). The measurement of temperature is done at intervals of one minute for the whole test period of five hours. The readings of thermocouples are delivered to a digital data logger for later analysis. The collector inlet and outlet temperature are used to estimate the thermosyphonic mass flow rate using the proposed equation (eq. 1). This is the experimental value which is compared to the analytical value estimated using the computer software.

## 5. Numerical Modeling

The thermal performance of the system is investigated by calculating the temperature distribution at all parts of the thermosyphon loop. This process is accomplished using the commercial software ANSYS-FLUENT 14. The whole length of the loop is discretized to large number of nodes (2.5 – 5.2 million nodes).

Grid and time independency tests are carried out to verify the choice of the suitable number of grids and the time step used in the simulation. Tables (2 & 3) illustrate the results of these tests. It can be seen that doubling the number of grids from 2.5 million to 5.2 million does not greatly influence the results. However, doubling the time step has more pronounced effect on the results. Accordingly, 2.5 million elements with 3 seconds time step were used in the simulation program.

*Table 2*

**Mesh independency tests results**.

| L/d ratio | Case | N. pipe | N. Element (million) | Temperature (ºC) | Difference in Temperature (%) |
|---|---|---|---|---|---|
| 50 | 1 | 5 | 2.5 | 15.0725 | |
| | | | 5.2 | 15.0441 | 0.188 |
| 75 | 2 | 5 | 3.2 | 15.0948 | |
| | | | 6.5 | 15.0803 | 0.0958 |
| | 3 | 7 | 3.8 | 15.0678 | |
| | | | 7.8 | 15.0852 | 0.1157 |
| | 4 | 9 | 4.4 | 15.0525 | |
| | | | 9.1 | 15.0778 | 0.1677 |
| 100 | 5 | 5 | 3.8 | 15.0873 | |
| | | | 7.8 | 15.1046 | 0.1145 |

*Table 3*

**Time independency tests results**.

| Time Step (sec.) | Temperature(ºC) | Difference in Temperature (%) |
|---|---|---|
| 3 | 31.585 | 0.08 |
| 6 | 31.61 | 0.5809 |
| 12 | 31.795 | |

## 6. Results and Discussion

### 6.1. Validation and Experimental Results

Tests were carried out for three patterns of artificial solar radiation, namely; constant, intermittent and real heat fluxes. Fig. 4. depicts the variations in temperatures at the collector inlet and outlet and inside the tank during five hours of exposure to a constant heat flux of 500 W/m$^2$. The selection of the constant value of heat flux is done to be consistent with the level of the real solar radiation at the sight of Huddersfield (UK). It is comparable to an average value of the varying solar radiation during a typical in March. This value is also used as an input value to the commercial software. Good agreement is achieved between numerical and experimental data which verifies the numerical procedure to be expanded for other operation conditions. However, the deviation increases with the elapse of time reaching maximum values of 8.28%, 10.17% and 9.86% for tank, collector inlet and outlet respectively at the end of the five hours. Fast increase in collector inlet and outlet temperatures is witnessed in the first 40 minutes, after which the increase slows down and takes linear increase at a rate of about 0.1°C/min. Tank temperature keeps a constant rate of increase during the whole simulation period reaching a maximum value of 34°C.

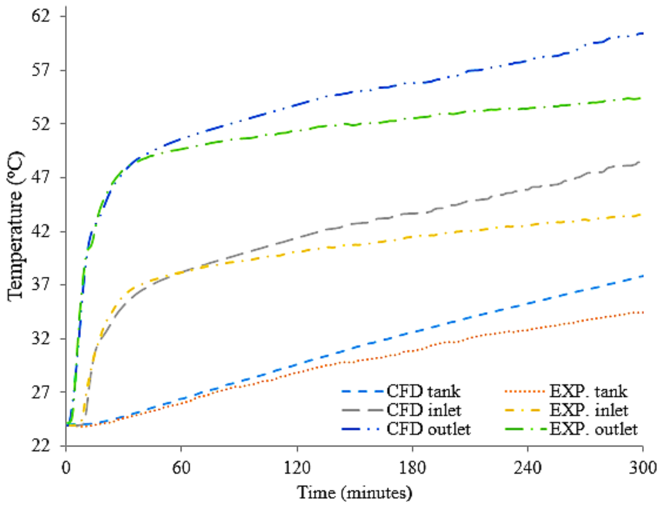


Fig. 4: Comparison between experimental and numerical results for a constant heat flux of 500 W/m$^2$

The variation of thermosyphonic mass flow rate during the five hours of constant heat flux is shown if Fig. 5. The mass flow rate increases rapidly in the first 40 minutes then tends to stabilize during the rest of simulation period around 0.0035kg/s. The calculated value of the mass flow rate is higher than the measured value. The reason is attributed to the absence of the minor losses terms in the mass flow rate formula which leads to a slight over estimation of the mass flow rate. The maximum error between calculated and measured values of mass flow rate is 18% at the start of simulation. The error stabilizes to about 9% for most of the test period.

The effect of intermittent heat flux was also considered in the present work. This situation resembles the discontinuity of solar radiation due to the presence of clouds. Table 4 represents a hypothetical case of intermittent solar radiation (heat flux) where the power to the solar simulator (which is the source of heat flux) was switched off for 15 minutes every 90 minutes of constant heat flux of 500 W/m$^2$.

*Table 4*

**Intermittent heat flux pattern**

| Time (minutes) | 0-90 | 90-105 | 105-195 | 195-210 | 210-300 | 300-315 | 315-405 | 405-420 |
|---|---|---|---|---|---|---|---|---|
| Heat flux (W/m$^2$) | on | Off | on | off | on | off | On | off |

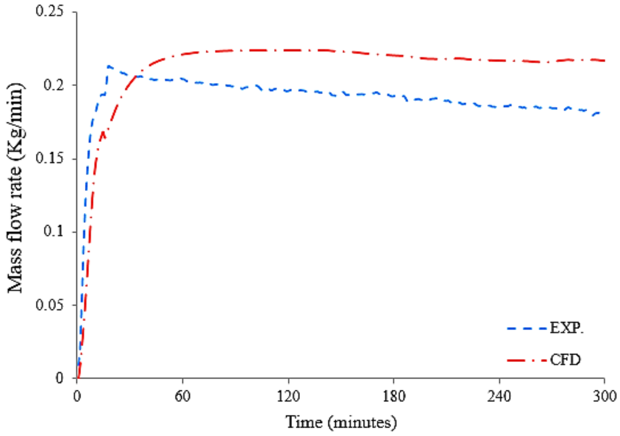


Fig. 5: Comparison between measured and estimated mass flow rate.

Fig. 6 shows the variation of tank, collector inlet and outlet temperature subjected to the intermittent heat flux pattern of table 4. The absence of the heat flux caused a sharp decrease in collector inlet and outlet temperature. However, the effect is marginal on the tank temperature which kept increasing till the end of the test period.

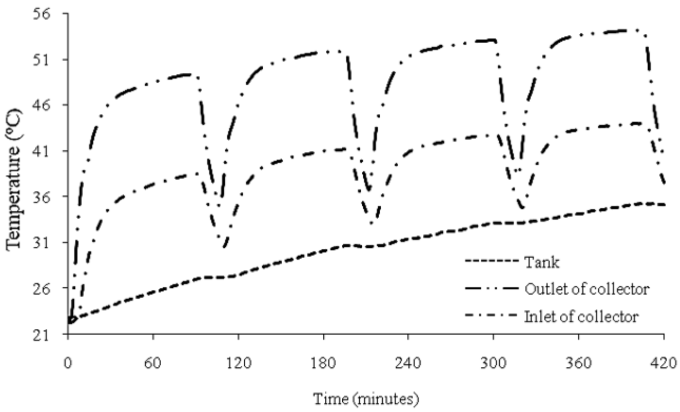


Fig. 6: Variation of temperatures in the system for the case of intermittent heat flux.

A significant decrease in thermosyphonic mass flow rate accompanied the absence of heat flux as can be seen in Fig.7. This effect indicates that the heat flux constitutes a considerable part of the driving mechanism in any natural circulation loop.

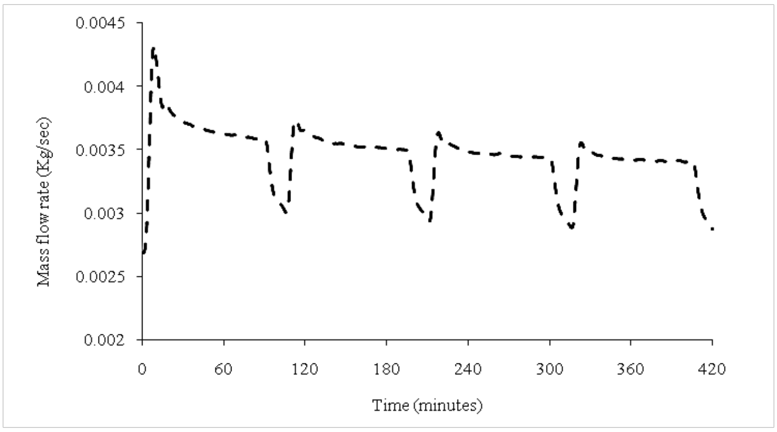


Fig. 7: Variation of the mass flow rate in the system for the case of intermittent heat flux.

## 6.2. Numerical Results

### Effect of Tilt Angle

The simulation is then carried out numerically for a real pattern of heat flux. The pattern is carefully chosen to resemble the solar radiation at the site of Huddersfield (UK) on 15th of March. Three different tilt angles are used to ascertain the best one of them. It is evident from Fig. 8 that 53° tilt angle make the collector receive the maximum solar radiation. This result is compatible with the popular "role of thumb" of aligning the collector at a tilt angle equals to the latitude of the site. This value is used in all calculations and test in the present study.

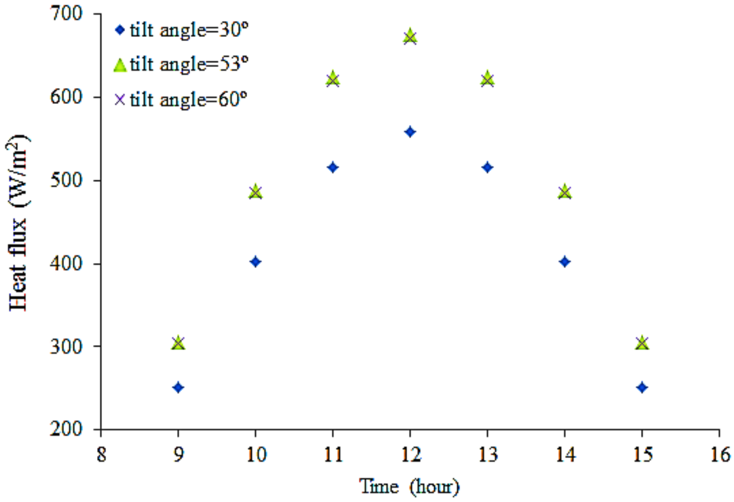


Fig. 8: Variation of heat flux for three tilt angles for the characteristic day 15th of March.

**Effect of Number of Riser Pipes**

Fig. 9 shows the variation of tank temperature during the simulation period for different number of risers. It can be seen that the number of risers has marginal effect on the tank temperature which not exceeds 4°C at the end of simulated period. Increasing number of risers increases tank temperature for the same collector area because the risers become more effective in cooling the absorber plate and hence collecting more heat. The mass flow rate at each pipe is decreased for more risers causing a reduction in frictional losses. However, the total mass flow rate of all risers increases with the increase in the number of risers as can be seen from Fig. 10. The profile of change in mass flow rate follows the change in heat flux during the simulated period. This fact further proves the dependency of mass flow rate on the heat flux.

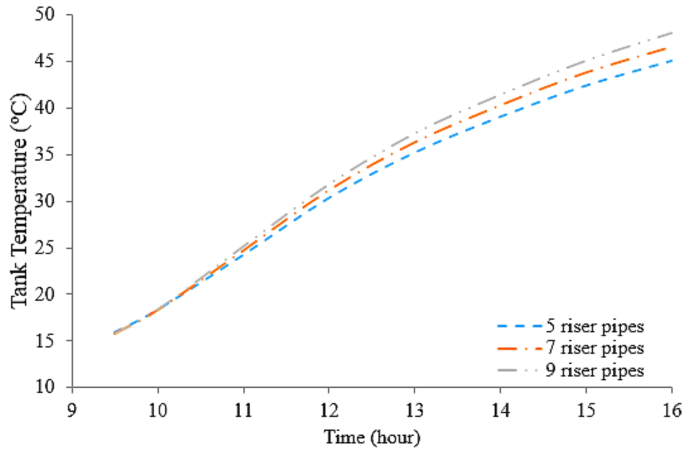


Fig. 9: Variation of tank temperature for different number of risers on 15th of March.

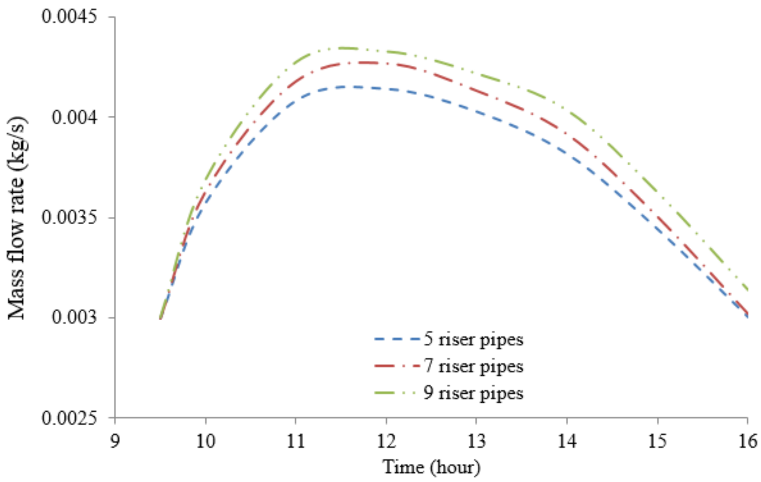


Fig. 10: Variation of thermosyphonic mass flow rate for different number of risers on 15th of March.

**Effect of L/d Ratio**

Simulations are also carried out to consider the effect of riser length to its diameter (L/d). It can be seen from Figure (11) that increases (L/d) ratio causes a considerable increase in tank temperature. When a long riser with small diameter is employed (high L/d), the fluid inside the riser has more time to collect energy from the absorber plate which is translated as an increase in tank temperature. The thermosyphonic mass flow rate also increases with increased (L/d) ratio as shown in Fig. 12. The higher temperature at the end of a longer riser causes further decrease in density leading to an increase in the driving potential between the cold tank and hot solar collector.

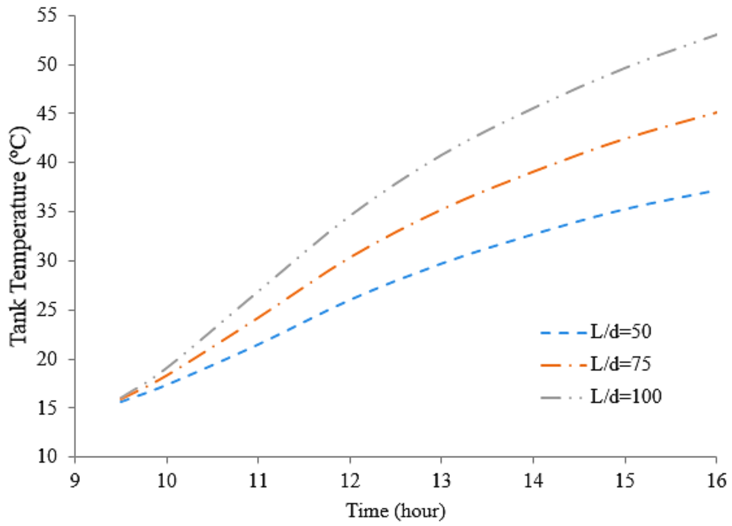


Fig. 11: Variation of tank temperature for three different length-to-diameter ratios.

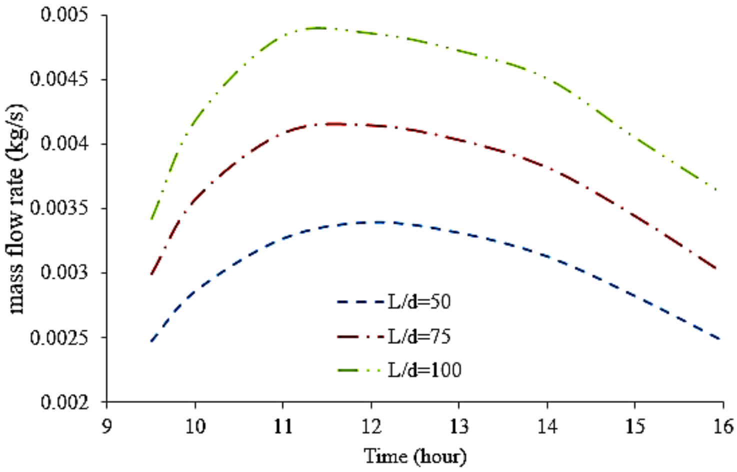


Fig. 12: Variation of mass flow rate for three different length-to-diameter ratios.

## 7. Conclusions

An experimental and numerical study was carried out on a thermosyphon solar water heater. Water is the working fluid that flows in a closed loop to convey the collected solar energy from the flat-plate solar collector to a heat exchanger immersed inside the water storage tank. The tests were carried out indoor using four Halogen lamps to supply artificial solar radiation on the collector surface. The following conclusions can be drawn from the present study:-

a) Exposing the system to a constant value of heat flux of 500 W/m$^2$ for five hours made the tank reach a maximum temperature of 34$^o$C at the end of test period.

b) The constant value of heat flux keeps the thermosyphonic mass flow rate approximately constant around 0.0035 kg/s during most of the test period.

c) The effect of intermittent solar radiation is marginal on tank temperature which keeps increasing, yet, at a lower rate.

d) Increasing the number of risers for a constant collector area has a marginal effect on tank temperature.

e) Increasing riser length to diameter ratio causes a considerable increase in tank temperature.

**Nomenclature**

| | |
|---|---|
| D | riser diameter (m) |
| $\dot{m}$ | thermosyphonic mass flow rate (kg/s) |
| $T_{in}$ | collector inlet temperature ($^o$C) |
| $T_{out}$ | collector outlet temperature ($^o$C) |
| $T_p$ | collector plate temperature ($^o$C) |
| L | riser length (m) |
| $\mu$ | kinematic viscosity (Pa.s) |

**Acknowledgement**

The authors wish to express their deep thanks and gratitude to the support provided by (Al-Mustansiriyah University) to accomplish the present work.

R E F E R E N C E S

[1] *D.J. Close*, The Performance of Solar Water Heaters with Natural Circulation, Solar Energy,**6**(1), 1962, pp. 33-40.

[2] *C.L. Gupta and H.P. Garg*, System Design in Solar Water Heaters with Natural Circulation, Solar Energy,**12**, 1968, pp. 163-182.

[3] *K.S. Ong*, A Finite Difference Method to Evaluate the Performance of a solar energy water heater, Solar Energy, **16**, 1974, pp. 131-147.

[4] *K.S. Ong*, An Improved Computer Program for the Thermal Performance of a Solar Water Heater, Solar Energy, **18**, 1976, pp. 183-191.

[5] *G.L. Morrison and D.B.J. Ranatunga*, Thermosyphon Circultion in Solar Collectors, Solar Energy,**24**, 1980, pp. 191-198.
[6] *B.J. Huang*, Similarity Theory of Solar Water Heater with Natural Circulation, Solar Energy,**25**, 1980, pp. 105-116.
[7] *A. Mertol, W. Place, T. Webster and R. Greif*, Detailed Loop Model (DLM) Analysis of Liquid Solar Thermosyphons with Heat Exchangers, Solar Energy,**27**, 1981, pp. 367-386.
[8] *G.L. Morrison and J.E. Braun*, System Modelling and Operation Characteristics of Thermosyphon Solar Water Heaters, Solar Energy,**34**, 1985, pp. 389-405.
[9] *P.A. Hobson and B. Norton*, Verified Accurate Performance Simulation Model of Direct Thermosyphon Solar Energy Water Heaters, ASME J. of Solar Energy Engineering,**110**, 1988, pp. 282-292.
[10] *B.J. Huang*, Performance rating method of thermosyphon solar water heaters, Solar Energy, **50**(5), 1993, pp. 435-440.
[11] *G.L. Morrison, A. Nasr, M. Behnia and G. Rosengarten*, Analysis of horizontal mantle heat exchangers in solar water heating systems, Solar Energy, **64**(1-3), 1998, pp. 19-31.
[12] *V. Belessiotis and E. Mathioulakis*, Analytical approach of thermosyphon solar domestic hot water system performance, Solar Energy, **72**(4), 2002,pp. 307-315.
[13] *P.M.E. Koffi, H.Y. Andoh, P. Gbaha, S. Toure andG. Ado*, Theoretical and experimental study of solar water heater with internal exchanger using thermosiphon system, Energy Conversion and Management, **49**, 2008, pp. 2279-2290.
[14] *S. Kalogirou*, Thermal performance, economic and environmrntal life cycle analysis of thermosiphon solar water heaters, Solar Energy, **83**, 2009, pp. 39-48.
[15] *J. Subramanian, S. Tamilkozhndu, and T. Selvam*, Experimental Studies on Variable Header Solar Water Heating System. in 2nd International Conference on Mechanical, Production and Automobile, 2012.
[16] *K. Zelzouli, A. Guizani and C. Kerkeni*, Numerical and experimental investigation of thermosyphon solar water heater, Energy Conversion and Management, **78**, 2014, pp. 913-922.
[17] *K.K. Tse and T.T. Chow*, Dynamic model and experimental validation of an indirect thermosyphon solar water heater coupled with a parallel circular tube rings type heat exchange coil, Solar Energy, **114**, 2015, pp. 114-133.
[18] *M. Srivinas*, Domestic solar hot water systems: developments, evaluations and essentials for "viability" with a special reference to India, Renewable and Sustainable Energy Reviews, **15**, 2011, pp. 3850-3861.
[19] *B. Kundu*, Performance analysis and optimization of absorber plates of different geometry for a flat-plate solar collector: a comparative study, Applied Thermal Engineering,**22**(9), 2002, pp. 999-1012.
[20] *Y. Varol and H.F. Oztop*, A comparative numerical study on natural convection in inclined wavy and flat-plate solar collectors, Building and Environment,**43**(9), 2008, pp. 1535-1544.
[21] *P. Sivakumar et al.*, Performance improvement study of solar water heating system, ARPN Journal of Engineering and Applied Sciences,**7**(1), 2012, pp. 45-49.
[22] *K. Amori and N. Jabouri*, Thermal performance of solar hot water systems using a flat plate collector of accelerated risers, The Journal of Engineering Research,**9**(1), 2012, pp. 1-10.